Monatsh Chem (2011) 142:907–916
DOI 10.1007/s00706-011-0507-5

ORIGINAL PAPER

Synthesis, characterization, and optical properties of 2-amino-4-aryl-6-(9,9′-spirobifluoren-2-yl)pyrimidines

Yingbo Shi · Qiancai Liu · Jie Tang

Received: 23 November 2010 / Accepted: 14 April 2011 / Published online: 19 May 2011

Abstract A series of 2-amino-4-aryl-6-(9,9′-spirobifluoren-2-yl)pyrimidines have been synthesized by the reaction of guanidine and chalcones under basic conditions. The physical and optical properties indicated that these compounds generally show good blue light emissions and excellent thermal stabilities. Intermolecular hydrogen bonds and interactions have strong influences on their properties.

Keywords Synthesis · Pyrimidine · Spirobifluorene · Fluorescence

Introduction

Organic π-conjugated oligo- and poly(aryl/heteroaryl) systems have attracted numerous attention due to their potential utilization as components of organic light-emitting devices (OLEDs) for flat displays and lightening [1]. In organic electroluminescent materials, non-planar structures of precursors can effectively prevent the formation of crystals [2] and increase molecular amorphism.

Materials with spirobifluorene moieties have been considered promising candidates for blue-light-emitting materials in both small-molecule- and polymer-based devices [3–5]. Tour et al. reported spirobifluorene derivatives as electroluminescent materials in 1996 [6]; subsequently numerous research results have been reported about blue-light-emitting materials comprising spirobifluorene derivatives, such as anthracene-spirobifluorenes, dispirobifluorenes, and pyrene-substituted spirobifluorenes [7–12]. Pyrimidine derivatives combined with a spirobifluorene subunit could be useful in such materials as a result of their high electron affinity and lack of *ortho–ortho* C–H interactions. For example, good efficiency, stability, and excellent solubility of 2,7-bis[2-(4-*t*-butylphenyl)pyrimidin-5-yl]-9,9′-spirobifluorene (TBPSF) render it a pure blue light emitter [13]. On the other hand, the 2-amino group and nitrogen on the pyrimidine ring could be used as probes for the recognition of different species on the basis of host–guest interactions such as hydrogen bonding and van der Waals interactions with other functional groups. Aminopyrimidine derivatives have been used in supramolecular assembly [14], as fluorescent probes [15, 16], and in studying in vitro antibacterial activity [17–20].

We envisioned that novel compounds with unique properties should be accessible by combining spirobifluorene with various pyrimidine subunits. It is worthwhile to develop a strategy for the preparation of novel and versatile functionalized pyrimidine-based oligo(arylenes) by well-defined synthetic routes. This prompted us to explore these types of new compounds which could be potentially used as precursors for organic light-emitting diodes (OLEDs) [13]. The spirobifluorene motif was chosen because of its high stability and good luminescence efficiency as described above; other aryl groups such as phenyl, thienyl, and naphthyl were used to investigate the influence of substituents on the motif's fluorescence properties. Furthermore, the whole system might be further used as a fluorescent sensor for biologically active compounds such as peptides, nucleic acids, and proteins by introducing suitable substituents on the pyrimidine skeleton. In this paper, we report the synthesis, characterization, and optical properties of 2-amino-4-aryl-6-(9,9′-spirobifluoren-2-yl)pyrimidines **6a–6e** (Scheme 1).

Y. Shi · Q. Liu (✉) · J. Tang
Department of Chemistry, East China Normal University, Shanghai 200062, China
e-mail: qcliu@chem.ecnu.edu.cn

Scheme 1

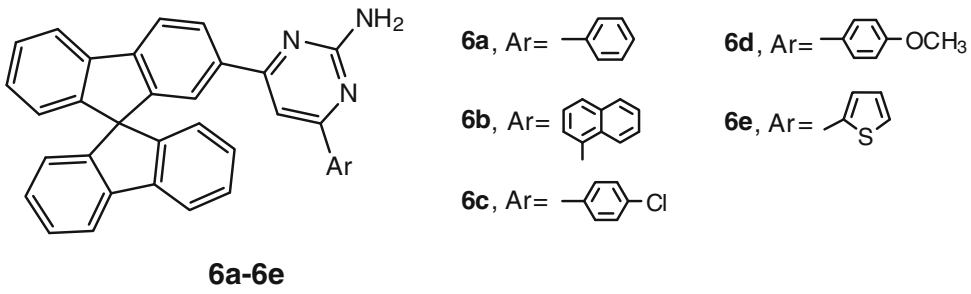

6a-6e

Results and discussion

Synthesis

Generally 2-amino-4,6-diarylpyrimidines could be synthesized from either chalcones, 1,3-dicarbonyl compounds, or β-alkynone condensation with guanidine salt under reflux or microwave-assisted conditions [21–28]. They can also be synthesized by palladium-catalyzed cross-coupling reaction of 4,6-dihalogenated pyrimidines and arylboronic acids [29, 30]. However, the syntheses from 1,3-dicarbonyl compounds and β-alkynones such as $ArC{\equiv}CCOAr'$ are evidently more difficult and complex than those from chalcones. The synthetic routes for compounds **6a**–**6e** are illustrated in Scheme 2 and used the reaction of chalcones and aldehydes, which is transition metal catalyst free. Compounds **6a**–**6e** were synthesized starting with 9,9′-spirobifluorene (**3**), which was obtained by the reaction of the Grignard reagent of 2-bromobiphenyl (**1**) with 9-fluorenone initially to form tertiary alcohol **2**, followed by the ring closure in HOAc with acid as catalyst [31]. The aldol condensation of 2-acetyl-9,9′-spirobifluorene (**4**), formed by Friedel–Crafts acylation of **3** [32, 33], with aromatic aldehydes under basic conditions afforded chalcones **5a**–**5e** in excellent isolated yields (80–90%). The ring closure of chalcones and guanidine nitrate in the presence of base was conducted by refluxing for 24 h to afford **6a**–**6e**. The products generally show high decomposition temperatures or melting points which depend strongly on the substituents present; the melting point of **6b** is the lowest, whereas that of **6e** is the highest (Table 2).

The structures of the compounds described above were assigned by NMR spectroscopy, mass spectrometry, and elemental analyses. In addition, the structures of **6a**, **6b**, and **6e** were further confirmed by X-ray diffraction (Fig. 1).

Single-crystal X-ray determination

As a result of the good solubilities of **6a**, **6b**, and **6e** in organic solvents, crystals that were of sufficient quality for X-ray structure determination were obtained from CH_2Cl_2/EtOH. Single-crystal X-ray analyses of **6a**, **6b**, and **6e** confirmed the substitution patterns in accordance with their NMR spectra. The results are shown in Fig. 1 and Tables 1 and 2.

It is quite interesting that strong hydrogen bonds between the 2-aminopyrimidine skeleton and aromatic pendants on the pyrimidine ring, π–π interactions, and C–H$\cdots\pi$ effects in **6a**, **6b**, and **6e** were found, which might have a strong impact on the conjugate planes (Fig. 1, Table 1). In the case of **6e**, there are four hydrogen bonds

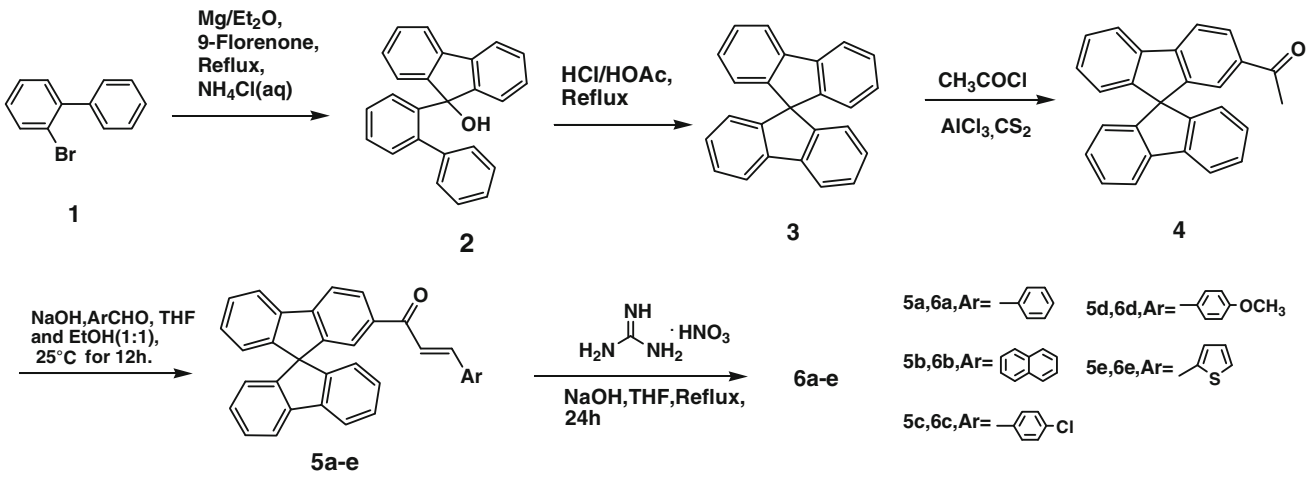

Scheme 2

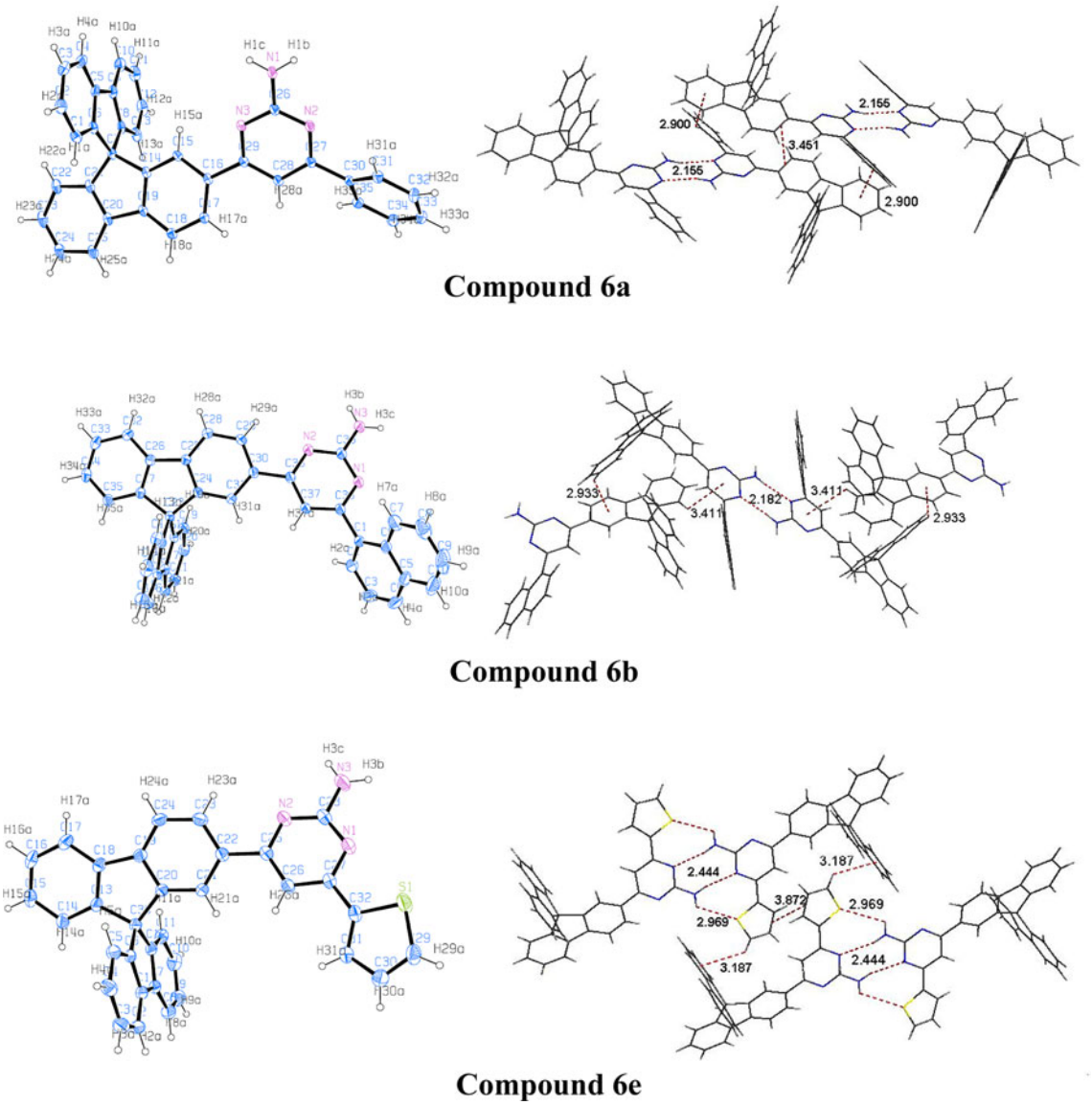

Fig. 1 Crystal structures, hydrogen bonds, π–π interactions, and C–H···π effect of **6a**, **6b**, and **6e**

Table 1 Hydrogen bonds and dihedral angles between the aryl and pyrimidine rings of **6a**, **6b**, and **6e**

	Hydrogen bond data (length and angle)	Dihedral angle (°) between the aryl and pyrimidine ring
6a	N1A–H1BA···N2, 2.15 Å, 165.71°	38.62
6b	N3A–H3CA···N1, 2.18 Å, 167.35°	58.96
6e	N3A–H3BA···N1, 2.44 Å, 158.84°	17.08
	N3A–H3CA···S1, 2.97 Å, 102.17°	

between the two molecules, which could explain why the melting point of **6e** is the highest. Comparing the dihedral angles between the aryl and pyrimidine rings, **6b** has a larger steric hindrance which might be responsible for the lowest yield.

The intermolecular hydrogen bonds, π–π interactions, and C–H···π effects found in this kind of compound could be considered as sites for selective recognition of different species towards supramolecular assembly and fluorescent probe studies [7, 8].

UV–vis and fluorescence spectra

The UV–vis spectra of compounds **6a–6e** are shown in Fig. 2. These spectra exhibited similar absorption peaks at 280–360 nm as a result of the compounds' structural similarities. The absorptions from $\pi \rightarrow \pi^*$ transitions for **6a–6d** in CH_2Cl_2 (DCM) are centered at 344–345 nm,

Table 2 Crystal data for compounds **6a**, **6b**, and **6e**

	6a	**6b**	**6e**
Empirical formula	$C_{35}H_{23}N_3{\cdot}CH_2Cl_2$	$C_{39}H_{25}N_3{\cdot}CH_2Cl_2$	$C_{33}H_{21}N_3S$
Molecular weight	568.47	618.53	491.59
Description	Colorless diamond	Colorless diamond	Colorless diamond
Size (mm^3)	0.47 × 0.29 × 0.27	0.874 × 0.507 × 0.314	0.264 × 0.127 × 0.091
Temperature (K)	173(2)	296(2)	296(2)
Crystal system	Monoclinic	Monoclinic	Monoclinic
Space group	*P*-1	*P*2(1)/*n*	*C*2/*C*
a (Å)	9.3186(4)	8.9752(3)	23.2902(3)
b (Å)	12.4707(5)	32.4381(12)	11.8235(2)
c (Å)	13.2568(4)	11.3700(4)	17.7942(2)
α (°)	106.758	90	90
β (°)	93.777	103.38	100.20
γ (°)	102.681	90	90
V ($Å^3$)	1425.33(9)	3141.43(19)	4822.59(12)
Z	2	4	8
Calculated density (mg m^{-3})	1.325	1.308	1.354
Scan mode	*φ*- and *ω*-scans	*φ*- and *ω*-scans	*φ*- and *ω*-scans
F(000)	588	1,280	2,048
Absorption coefficient (mm^{-1})	0.259	0.241	0.163
θ range (°)	1.62–25.01	1.99–25.00	1.78–25.01
Index ranges	$-11 \le h \le 11$	$-10 \le h \le 10$	$-27 \le h \le 27$
	$-14 \le k \le 14$	$-38 \le k \le 36$	$-14 \le k \le 14$
	$-15 \le l \le 15$	$-13 \le l \le 13$	$-21 \le l \le 21$
Reflections collected	16,654	35,929	37,598
Independent reflections	4,993 [*R*(int) = 0.0237]	5,534 [*R*(int) = 0.0213]	4,260 [*R*(int) = 0.0509]
Data/restraints/parameters	4,993/0/397	5,534/0/416	4,260/0/334
GOF on F^2 (all)	1.050	1.030	1.021
Final *R* ($I > 2\sigma(I)$)	*R*1 = 0.0622, *wR*2 = 0.1752	*R*1 = 0.0604, *wR*2 = 0.1641	*R*1 = 0.0424, *wR*2 = 0.1004
R indices (all data)	*R*1 = 0.0751, *wR*2 = 0.1887	*R*1 = 0.0663, *wR*2 = 0.1716	*R*1 = 0.0690, *wR*2 = 0.1178
Transmission (ratio of max to min)	0.9335 and 0.8881	1 and 0.884977	1 and 0.873919
Largest diff. peak (e $Å^{-3}$)	0.837	0.533	0.198
Largest diff. hole (e $Å^{-3}$)	−0.510	−0.825	−0.309

GOF goodness of fit

whereas that of **6e** is centered at 358 nm, i.e., with a 10-nm red shift relative to those of **6a**–**6d** (Table 3).

Their solution fluorescence spectra indicate that the emissions of compounds **6a**–**6e** (Fig. 3) are smooth and pure blue emissions could be obtained with peaks at 399–406 nm (Table 3). The emission wavelength of **6a** was the smallest (399 nm), whereas that of **6e** was the largest (406 nm). The differences of quantum yields among compounds **6a**–**6e** were studied with 9,10-diphenylanthracene as reference. The results indicated that **6b** and **6e** show good quantum yields (≥60%), whereas that of **6a** was the lowest (37%, Table 3). This might be explained by the steric hindrance of the naphthyl ring of **6b** and four hydrogen bond systems of **6e**, which could prevent the free rotation of naphthyl and thienyl groups and reduce the non-radiative transition between the molecules, thus improving the quantum yields.

The solid emissions of **6a**–**6e** (Fig. 4) peaked at 418–442 nm with a red shift of ca. 10–36 nm relative to their solution emissions. This behavior might be due to the effects of hydrogen bonds, π–π interactions, and C–H···π effects formed in the solid state.

*Thermostabilities of compounds **6a**, **6b**, and **6e***

The thermal properties of **6a**, **6b**, and **6e** were investigated by thermal gravimetric analysis (TGA) and differential scanning calorimetry (DSC). Compounds **6a**, **6b**, and **6e**

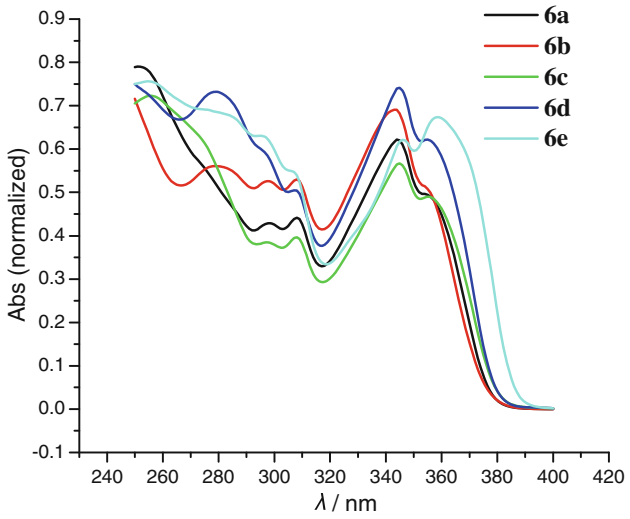

Fig. 2 UV–vis absorption spectra of **6a–6e** (1×10^{-6} M, DCM)

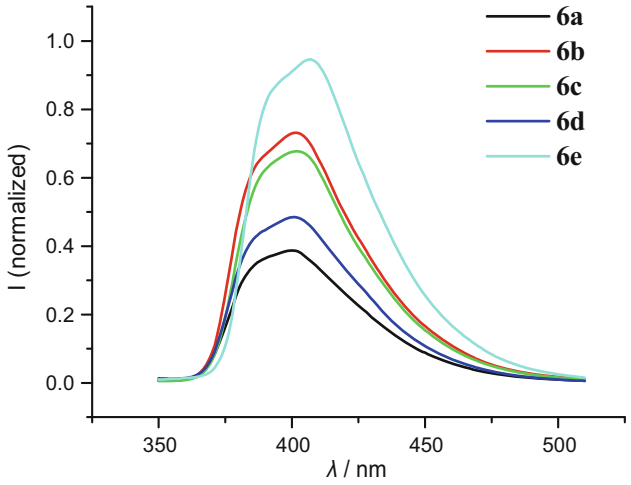

Fig. 3 Solution fluorescence emission spectra of **6a–6e** (1×10^{-6} M, DCM)

exhibited excellent thermal stabilities. The decomposition temperatures (T_d) with 5% weight loss under a N_2 atmosphere of **6a**, **6b**, and **6e** are quite high (382 °C for **6a**, 383 °C for **6b**, 381 °C for **6e**). The DSC curves of **6a**, **6b**, and **6e** showed obviously crystalline melting temperatures ranging from 180 °C (**6b**) to 307 °C (**6e**).

HOMO/LUMO and electrochemistry studies

Cyclic voltammetry (CV) and calculations by Gaussian 03 at B3LYP/6-31G* level are both useful tools for studying the front orbital energies. Cyclic voltammetry data indicated that **6a**, **6b**, and **6e** have good electrochemical stabilities in the reduction area, but no reversible process was observed in the oxidation which might be due to the amino groups on the pyrimidine rings (Fig. 5).

The oxidation process for **6a**, **6b**, and **6e** occurs at 1.96, 1.90, and 1.82 eV, respectively, whereas the reversible single-electron reduction occurs at −1.43, −1.46, and −1.44 eV; therefore the HOMO/LUMO energy levels from CV were estimated as −5.93, −5.87, and −5.79, and −2.54, −2.51, and −2.53 eV, respectively. Calculation results show that the HOMO/LUMO energy levels of **6a**, **6b**, and **6e** from density functional theory (DFT) calculations were estimated as −5.63, −5.62, and −5.63, and −1.57, −1.59, and −1.66 eV, respectively (Table 4). The large variations between the experimental and calculated LUMO data might be due to the different calculation methods and conditions. The LUMO data from the CV were calculated from experiential equation and the DFT calculation was based on Koopmans' theorem which ignores the electron gain and loss effect of other electrons. On the other hand, the HOMO/LUMO energies of **6a**, **6b**, and **6e** were close to that of tris(8-hydroxyquinoline)aluminum(III) (Alq_3; −5.62/−2.85 eV) [34]. Thus the differences of orbital energy among these compounds from

Table 3 Optical data and thermoanalysis data of **6a–6e**

	λ_{abs} (max) (nm)[a]	$\lambda_{em,solution}$ (nm)[a]	$\lambda_{em,\ solid}$ (nm)[b]	Φ (%)[c]	T_m (°C)[d]	T_d (°C)[e]
6a	344	399	418	37	256	382
6b	343	404	443	60	180	383
6c	345	401	416	45	291	–
6d	345	400	428	43	230	–
6e	358	406	442	63	307	381

[a] In dichloromethane (1.0×10^{-6} M)

[b] The solid emission spectrum was measured with solid powder

[c] The relative quantum yield Φ was measured using standard procedures with reference to 9,10-diphenylanthracene (1.0×10^{-6} M in cyclohexane, Φ = 90%)

[d] **6a**, **6b**, and **6e** data obtained from differential scanning calorimetry (DSC); **6c** and **6d** data obtained from a micrographic measuring apparatus

[e] Decomposition temperature T_d is defined as the temperature at which 5% loss occurs during heating

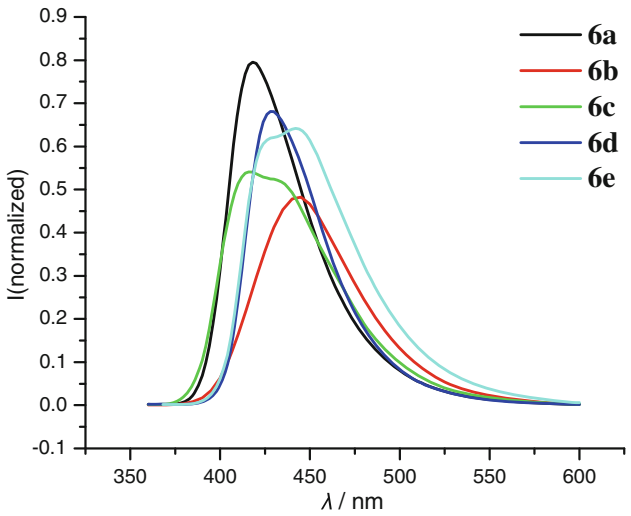

Fig. 4 Solid fluorescence emission spectra of **6a**–**6e**

HOMO/LUMO data lead to good feasibilities as electron transport materials. The similar electrochemical band gaps of compounds **6a**, **6b**, and **6e** range from 3.26 to 3.38 eV (366–379 nm), which are in accordance with their UV–vis spectra. Both the electrochemical band gaps and theoretical calculation values (4.23–4.56 eV) are also close to the energy band gaps of other blue-emitting materials [35]. Visual frontier molecular orbitals of **6a**, **6b**, and **6e** were also established (Fig. 6).

Conclusion

We have successfully synthesized a series of 2-amino-4-aryl-6-(9,9′-spirobifluoren-2-yl)pyrimidines. Their optical properties indicated that some of them might be used as precursors for novel blue-light-emitting materials (with quantum yields ranging from 37 to 63%). The intermolecular interactions, hydrogen bonds, and C–H···π effects found in these molecules might be considered as versatile tools for molecular recognition and luminescent probes. Further studies are underway to establish the potential utilization of the title compounds in the fields of OLED devices and molecular recognition.

Experimental

9,9′-Spirobi[9*H*-fluorene] (**3**) was prepared according to [31]. Commercially available reagents, solvents, and other materials were used without further purification other than stated below. THF was distilled from Na/benzophenone prior to use. Petroleum ether refers to the fraction with b.p. 60–90 °C. All operations were performed by standard Schlenk techniques unless otherwise stated. TLC was carried out by using silica gel 60 GF 254 and visualized under UV light (254 and 365 nm). Melting points were measured on an X-4 micrographic measuring apparatus. ^{1}H and ^{13}C NMR spectra were measured on a Bruker DRX 500

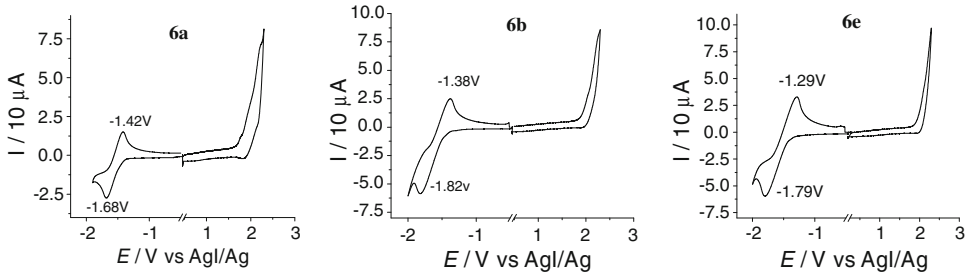

Fig. 5 Cyclic voltammograms of **6a**, **6b**, and **6e**. Anodic oxidation of a 2×10^{-3} M solution in CH_2Cl_2 + 0.1 M Bu_4NPF_6, 100 mV/s; cathode reduction of a 2×10^{-3} M solution in tetrahydrofuran (THF) + 0.1 M Bu_4NPF_6, 100 mV/s

Table 4 Electrochemical properties and HOMO/LUMO levels of **6a**, **6b**, and **6e**

	Electrochemical data					Calculation data		
	E_{Ox} (V)[a]	E_{Red} (V)[b]	HOMO (eV)[c]	LUMO (eV)[d]	ΔE^{el} (eV, nm)[e]	HOMO^{cal} (eV)[f]	LUMO^{cal} (eV)[f]	ΔE^{cal} (eV)[f]
6a	1.96	−1.43	−5.93	−2.54	3.38, 366	−5.63	−1.57	4.06
6b	1.90	−1.46	−5.87	−2.51	3.36, 368	−5.62	−1.59	4.03
6e	1.82	−1.44	−5.79	−2.53	3.26, 380	−5.63	−1.66	3.97

[a] In CH_2Cl_2

[b] In THF

[c] From the onset oxidation potential

[d] From the reduction potential

[e] ΔE^{el} = |HOMO − LUMO|; $\lambda = h\nu/\Delta E^{el}$ (eV) = 1,237.5/ΔE^{el} (nm) from redox data

[f] Using Gaussian 03 B3LYP/6-31G* calculation on models of the CIF documents; ΔE^{cal} = |HOMO − LUMO|

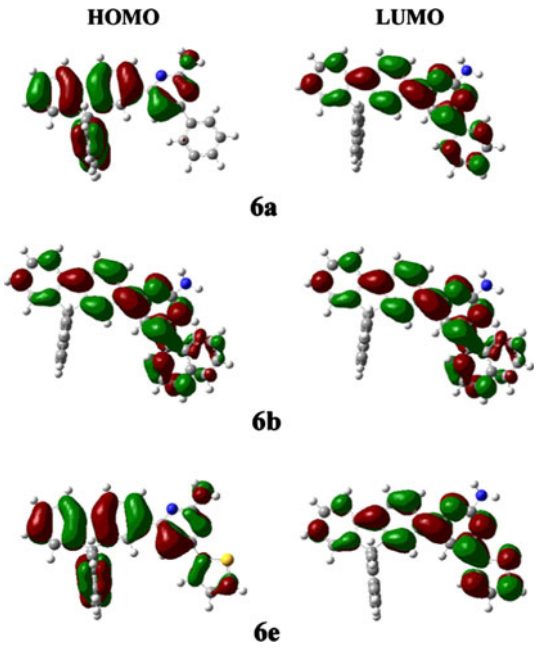

Fig. 6 Visual frontier molecular orbitals of compounds **6a**, **6b**, and **6e**

spectrometer (^{1}H NMR 500 MHz, ^{13}C NMR 125 MHz). Elemental analyses were measured on a Vario EL element analysis instrument. Mass spectra were recorded on an Angilent 5973 N mass spectrometer.

The crystal data were collected by a Bruker SMART CCD area detector with Mo Kα radiation ($\lambda = 0.71073$ Å). The structure solution and refinement was completed by Bruker SHELXTL [43]. The structures were solved by direct methods and refined by full-matrix least-squares on F^2 values of all data.

UV–vis spectra were recorded using a Carey-100 UV–vis spectrophotometer. Photoluminescence spectra were recorded at room temperature with an HITACHI F-4500 spectrofluorimeter using a xenon lamp. Quantum yields (Φ_{sol}) were calculated relative to 9,10-diphenylanthracene (1×10^{-6} M in cyclohexane, $\Phi_{sol} = 90\%$) by standard procedures. Φ_{sol} was determined according to the following equation [36, 37]:

$$\Phi_{sol} = \Phi_{ref} \times 100 \times \frac{(F_s \times A_r)}{(F_r \times A_s)} \times \left(\frac{n_s}{n_r}\right)^2$$

where subscripts "s" and "r" refer to the sample and reference, respectively. The integrated area of the emission peak in arbitrary units is given as F; n is the refractive index of the solvent ($n_s = 1.4244$ for DCM; $n_r = 1.4264$ for cyclohexane); and A is the absorbance. The emission spectra were recorded in solution in cyclohexane. The solid emission spectrum was measured from solid powders.

All electrochemical experiments were performed using a Pt disk electrode (diameter 1 mm), the counter electrode was a vitreous carbon electrode (diameter 3 mm), and the reference electrode was AgI/Ag. The redox cyclic voltammograms were measured with a electrochemical workstation (CH Instruments CHI-840C); the scan rate was 100 mV/s. All solvents were dried. The experiments were preceded by flushing with dry nitrogen gas for 5 min to remove oxygen in the system. With n-Bu_4NPF_6 (0.1 M) as supporting electrolyte, the oxidation processes were measured in CH_2Cl_2 and reduction processes were measured in THF. All samples were prepared as 2×10^{-3} M solutions. The ferrocene/ferrocenium (Fc^+/Fc) couple served as internal standard and all reported potentials are referenced to its reversible formal potential.

The HOMO and LUMO can be calculated according to the following equations [38]:

$$\text{HOMO} = [-(E_{Ox} - \Psi) - 4.8]\text{eV}$$
$$\text{LUMO} = [-(E_{Red} - \Psi) - 4.8]\text{eV}$$
$$\Delta E^{el} = |\text{HOMO} - \text{LUMO}|$$

where Ψ is the onset potential of ferrocene (Fc^+/Fc) versus AgI/Ag and equals 0.6761 V; E_{Ox} is the onset potential of the oxidation process; E_{Red} is the onset potential of the reduction process; 4.8 is the vacuum energy level of ferrocene.

Density functional theory (DFT) calculations were performed with the hybrid Becke-3 parameter exchange functional and the Lee–Yang–Parr nonlocal correlation functional (B3LYP) [39–42] implemented in Gaussian 03 (Revision B.01) using the 6-31G* basis set.

Thermogravimetric analyses (TGA) were performed with a Thermal analyzer Mettler Toledo TGA851e/SF/1100 under a nitrogen atmosphere. TGA measurements were carried out between 20 and 800 °C with a heating rate of 10 °C/min. The differential scanning calorimetry (DSC) data were collected from the heat process analysis.

1-(9,9′-Spirobi[9H-fluoren]-2-yl)ethanone (**4**)

To a two-necked round-bottom flask was added 6.2 g anhydrous $AlCl_3$, 2.17 g spirobifluorene **3** (6.9 mmol), and 30 cm^3 CS_2. Then a solution of 0.56 g acetyl chloride (7.1 mmol) in 10 cm^3 CS_2 was added dropwise with stirring within 10 min. The reaction mixture was heated at reflux for 2 h and then cooled to room temperature, followed by pouring into in a mixture of 100 cm^3 ice-cold water and 50 cm^3 2 N HCl. The mixture was extracted with dichloromethane (3×20 cm^3). The combined organic phase was dried over Na_2SO_4 and the solvent was evaporated. The residue was purified by column chromatography with dichloromethane and petroleum ether (4:1) to afford **4** in 1.60 g yield (65%). M.p.: 223–224 °C (m.p. 225 °C [21–28]).

*General procedure for preparation of **5a–5e***

To a flask was charged 1.79 g 2-acetylspirobifluorene **4** (5 mmol), the appropriate aldehyde (5.1 mmol), a mixture of THF and EtOH (4:1, 100 cm^3), and 10 cm^3 30% aq. NaOH solution. After stirring for 12 h at room temperature, the solution was neutralized by 2 N HCl, then the mixture was extracted with dichloromethane (3 × 20 cm^3), and the organic phase was dried over Na_2SO_4. After filtration and evaporation of the solvents, the products were purified by recrystallization from EtOH (80–90% yield).

3-Phenyl-1-(9,9′-spirobi[9H-fluoren]-2-yl)-2-propen-1-one (**5a**, $C_{34}H_{22}O$)
Yield 85%; m.p.: 194–196 °C; ^{1}H NMR (500 MHz, $CDCl_3$): $\delta = 7.97$ (d, $J = 8.0$ Hz, 1H), 7.93 (d, $J = 8.0$ Hz, 1H), 7.89 (d, $J = 8.0$ Hz, 2H), 7.71 (d, $J = 15.0$ Hz, 1H), 7.60–5.50 (m, 2H), 7.43–7.35 (m, 8H), 7.20 (t, $J = 7.5$ Hz, 1H), 7.14 (t, $J = 7.5$ Hz, 2H), 6.75–6.73 (m, 3H) ppm; ^{13}C NMR (125 MHz, $CDCl_3$): $\delta = 189.92$, 150.46, 149.45, 148.11, 146.70, 144.80, 142.17, 140.63, 137.94, 135.17, 130.61, 129.36, 129.21, 129.21, 129.08, 128.90, 128.66, 128.21, 124.58, 124.56, 124.46, 124.22, 122.42, 122.35, 121.41, 120.46, 120.21, 66.23 ppm.

3-Naphthyl-1-(9,9′-spirobi[9H-fluoren]-2-yl)-2-propen-1-one (**5b**, $C_{38}H_{24}O$)
Yield 80%; m.p.: 237–239 °C; ^{1}H NMR (500 MHz, $CDCl_3$): $\delta = 8.54$ (d, $J = 15.0$ Hz, 1H), 8.16 (dd, $J = 8.0$ Hz, $J = 2.5$ Hz, 1H), 8.13 (d, $J = 8.0$ Hz, 1H), 7.99 (d, $J = 8.0$ Hz, 1H), 7.93 (d, $J = 7.0$ Hz, 1H), 7.90–7.85 (m, 4H), 7.81 (d, $J = 7$ Hz, 1H), 7.56–7.38 (m, 8H), 7.18 (t, $J = 7.5$ Hz, 2H), 7.13 (t, $J = 7.5$ Hz, 2H), 6.76 (t, $J = 7.5$ Hz, 3H) ppm; ^{13}C NMR (125 MHz, $CDCl_3$): $\delta = 189.79$, 150.51, 149.48, 148.10, 146.80, 142.18, 141.66, 140.62, 137.93, 137.90, 133.92, 132.68, 131.95, 130.91, 130.87, 129.39, 129.33, 128.92, 128.24, 128.21, 127.16, 126.46, 125.62, 125.35, 125.16, 125.09, 124.62, 124.46, 124.24, 123.72, 121.16, 120.48, 120.31, 66.25 ppm.

3-(4-Chlorophenyl)-1-(9,9′-spirobi[9H-fluoren]-2-yl)-2-propen-1-one (**5c**, $C_{34}H_{21}ClO$)
Yield 86%; m.p.: 190–192 °C; ^{1}H NMR (500 MHz, $CDCl_3$): $\delta = 8.09$ (dd, $J = 8.0$ Hz, $J = 1.0$ Hz, 1H), 7.96 (d, $J = 8.0$ Hz, 1H), 7.92 (d, $J = 7.5$ Hz, 1H), 7.88 (d, $J = 7.5$ Hz, 2H), 7.63 (d, $J = 14.5$ Hz, 1H), 7.47 (d, $J = 8.0$ Hz, 4H), 7.42–7.30 (m, 6H), 7.18 (t, $J = 7.5$ Hz, 1H), 7.12 (t, $J = 7.2$ Hz, 2H), 6.77–6.74 (m, 3H) ppm; ^{13}C NMR (125 MHz, $CDCl_3$): $\delta = 189.92$, 150.48, 149.47, 148.08, 146.90, 143.31, 142.18, 140.56, 137.74, 136.52, 133.63, 129.87, 129.48, 129.39, 129.28, 128.28, 128.23, 124.57, 124.48, 124.26, 122.70, 121.23, 120.52, 120.32, 66.21 ppm.

3-(4-Methoxylphenyl)-1-(9,9′-spirobi[9H-fluoren]-2-yl)-2-propen-1-one (**5d**, $C_{35}H_{24}O_2$)
Yield 88%; m.p.: 179–181 °C; ^{1}H NMR (500 MHz, $CDCl_3$): $\delta = 8.10$ (dd, $J = 8.0$ Hz, $J = 1.5$ Hz, 1H), 7.96 (d, $J = 8.0$ Hz, 1H), 7.92 (d, $J = 7.5$ Hz, 1H), 7.89 (d, $J = 8.0$ Hz, 2H), 7.67 (d, $J = 15.5$ Hz, 1H), 7.51 (d, $J = 8.5$ Hz, 2H), 7.42–7.38 (m, 4H), 7.24 (d, $J = 15.5$ Hz, 1H), 7.18 (t, $J = 7.5$ Hz, 1H), 7.12 (t, $J = 7.5$ Hz, 2H), 6.89 (d, $J = 8.5$ Hz, 2H), 6.74 (t, $J = 10.5$ Hz, 3H), 3.83 (s, 3H) ppm; ^{13}C NMR (125 MHz, $CDCl_3$): $\delta = 189.95$, 161.81, 150.42, 149.33, 148.15, 146.51, 144.69, 142.16, 140.68, 138.22, 130.49, 129.30, 129.14, 128.20, 127.87, 124.50, 124.45, 124.26, 121.13, 120.47, 120.21, 119.99, 114.56, 66.20, 55.63 ppm.

1-(9,9′-Spirobi[9H-fluoren]-2-yl)-3-(2-thienyl)-2-propen-1-one (**5e**, $C_{32}H_{20}OS$)
Yield 90%; m.p.: 149–150 °C; ^{1}H NMR (500 MHz, $CDCl_3$): $\delta = 8.06$ (dd, $J = 7.5$ Hz, $J = 1.0$ Hz, 1H), 7.95 (d, $J = 8.0$ Hz, 1H), 7.91 (d, $J = 8.0$ Hz, 1H), 7.87 (d, $J = 7.0$ Hz, 2H), 7.89 (d, $J = 15.0$ Hz, 1H), 7.41–7.37 (m, 5H), 7.28 (d, $J = 3.0$ Hz, 1H), 7.19 (m, 2H), 7.11 (t, $J = 7.5$ Hz, 2H), 7.04 (t, $J = 4.0$ Hz, 1H), 6.75 (d, $J = 8.0$ Hz, 1H), 6.72 (d, $J = 8.0$ Hz, 2H) ppm; ^{13}C NMR (125 MHz, $CDCl_3$): $\delta = 189.31$, 150.46, 149.52, 148.10, 146.66, 142.17, 140.63, 137.89, 137.11, 131.95, 129.36, 129.08, 128.89, 128.49, 128.22, 128.17, 124.67, 124.21, 121.17, 121.14, 120.46, 120.15, 66.22 ppm.

*General procedure for preparation of **6a–6e***

A mixture of chalcone **5a**–**5e** (5 mmol) and guanidine nitrate (5 mmol) in 100 cm^3 THF and EtOH (4:1) was refluxed, while a solution of sodium hydroxide (0.4 mol) in 10 cm^3 water was added portionwise over 2 h. Refluxing was continued for further 24 h and the solution was neutralized by 2 N HCl. Then the mixture was extracted with dichloromethane (3 × 20 cm^3), and the organic phase was dried over Na_2SO_4. After filtration and evaporation of the solvents, the products were purified by column chromatography using dichloromethane and ethyl acetate (50:1).

4-Phenyl-6-(9,9′-spirobi[9H-fluoren]-2-yl)pyrimidin-2-amine (**6a**, $C_{35}H_{23}N_3$)
Yield 50%; $R_f = 0.34$; m.p.: 250–254 °C; ^{1}H NMR (500 MHz, $CDCl_3$): $\delta = 8.16$ (dd, $J = 8.5$ Hz, $J = 1.0$ Hz, 1H), 7.97 (t, $J = 8.0$ Hz, 2H), 7.96 (s, 1H), 7.91 (t, $J = 7.5$ Hz, 3H), 7.45–7.44 (m, 4H), 7.39 (t, $J = 7.7$ Hz, 3H), 7.28 (s, 1H), 7.16–7.11 (m, 3H), 6.77 (d, $J = 7.5$ Hz, 2H), 6.73 (d, $J = 7.5$ Hz, 1H), 5.04 (s, 2H) ppm; ^{13}C NMR (125 MHz, $CDCl_3$): $\delta = 166.35$, 160.00, 163.69, 150.03, 149.46, 148.60, 144.55, 142.12, 141.09, 138.02, 137.64, 130.53, 128.89, 128.71, 128.19, 128.09, 127.46, 127.34, 124.39, 124.30, 123.12, 120.70, 123.11,

120.44, 120.35, 104.44, 104.42, 66.32 ppm; EI-MS: $m/z = 485$ (100, M^+), 315 (20), 242 (19).

4-(1-Naphthyl)-6-(9,9′-spirobi[9H-fluoren]-2-yl)pyrimidin-2-amine (**6b**, $C_{39}H_{25}N_3$)
Yield 30%; $R_f = 0.38$; m.p.: >170 °C; ^{1}H NMR (500 MHz, $CDCl_3$): $\delta = 8.13$ (dd, $J = 8.0$ Hz, $J = 1.0$ Hz, 1H), 8.06 (d, $J = 8.0$ Hz, 1H), 7.95 (d, $J = 8.0$ Hz, 1H), 7.90–7.84 (m, 5H), 7.52–7.35 (m, 7H), 7.15–7.10 (m, 4H), 6.76 (d, $J = 7.5$ Hz, 2H), 6.73 (d, $J = 7.5$ Hz, 1H), 5.13 (s, 2H) ppm; ^{13}C NMR (125 MHz, $CDCl_3$): $\delta = 168.56$, 165.62, 163.38, 150.01, 149.60, 148.54, 144.65, 142.10, 141.09, 137.36, 137.20, 134.04, 130.82, 129.79, 128.76, 128.58, 128.17, 128.14, 127.47, 127.01, 126.88, 126.30, 125.67, 125.38, 124.34, 123.16, 120.73, 120.47, 120.39, 108.87, 108.84, 66.29 ppm; EI-MS: $m/z = 535$ (100, M^+), 491 (34), 315 (20), 245 (20), 220 (47).

4-(4-Chlorophenyl)-6-(9,9′-spirobi[9H-fluoren]-2-yl)pyrimidin-2-amine (**6c**, $C_{35}H_{22}ClN_3$)
Yield 58%; $R_f = 0.32$; m.p.: 290–291 °C; ^{1}H NMR (500 MHz, $CDCl_3$): $\delta = 8.37$ (d, $J = 8.0$ Hz, 1H), 8.20 (t, $J = 9.0$ Hz, 3H), 8.13 (d, $J = 7.0$ Hz, 1H), 8.07 (d, $J = 7.0$ Hz, 2H), 7.70 (s, 1H), 7.57 (s, 1H), 7.56 (d, $J = 4.0$ Hz, 2H), 7.44 (t, $J = 7.5$ Hz, 3H), 7.19–7.14 (m, 3H), 6.67 (d, $J = 7.0$ Hz, 4H), 6.62 (d, 1H) ppm; ^{13}C NMR (125 MHz, $CDCl_3$): $\delta = 165.08$, 164.49, 164.20, 149.89, 149.17, 148.66, 144.59, 142.07, 141.10, 137.50, 136.81, 135.86, 129.47, 129.28, 128.79, 128.27, 124.30, 124.11, 122.34, 121.87, 121.39, 102.32, 79.85, 66.24 ppm; EI-MS: $m/z = 519$ (100, M^+), 315 (32), 259 (37).

4-(4-Methoxyphenyl)-6-(9,9′-spirobi[9H-fluoren]-2-yl)pyrimidin-2-amine (**6d**, $C_{36}H_{25}N_3O$)
Yield 64%; $R_f = 0.34$; m.p.: 230–232 °C; ^{1}H NMR (500 MHz, $CDCl_3$): $\delta = 8.12$ (dd, $J = 8.0$ Hz, $J = 1.5$ Hz, 1H), 7.96–7.33 (m, 3H), 7.90 (t, $J = 8.0$ Hz, 3H), 7.42 (s, 1H), 7.38 (t, $J = 7.5$ Hz, 3H), 7.22 (s, 1H), 7.14–7.10 (m, 3H), 6.95 (d, $J = 9.0$ Hz, 2H), 6.76 (d, $J = 7.5$ Hz, 2H), 6.72 (d, $J = 7.5$ Hz, 1H), 5.03 (s, 2H), 3.84 (s, 3H) ppm; ^{13}C NMR (125 MHz, $CDCl_3$): $\delta = 165.74$, 163.66, 161.77, 149.98, 149.44, 148.61, 144.43, 142.12, 141.14, 137.83, 130.35, 128.87, 128.71, 128.22, 128.14, 128.10, 127.45, 142.41, 124.32, 123.09, 120.73, 120.46, 120.40, 114.25, 103.64, 66.30, 55.61 ppm; EI-MS: $m/z = 515$ (100, M^+), 315 (40), 257 (78).

4-(9,9′-Spirobi[9H-fluoren]-2-yl)-6-(2-thienyl)pyrimidin-2-amine (**6e**, $C_{33}H_{21}N_3S$)
Yield 66%; $R_f = 0.31$; m.p.: 307–309 °C; ^{1}H NMR (500 MHz, $CDCl_3$): $\delta = 8.10$ (d, $J = 8.0$ Hz, 1H), 7.96 (d, $J = 8.0$ Hz, 1H), 7.89 (t, $J = 7.5$ Hz, 3H), 7.68 (d, $J = 4.0$ Hz, 1H), 7.43–7.37 (m, 5H), 7.18 (s, 1H), 7.15–7.08 (m, 4H), 6.76 (d, $J = 7.5$ Hz, 2H), 6.73 (d, $J = 7.5$ Hz, 1H), 5.02 (s, 2H) ppm; ^{13}C NMR (125 MHz, $CDCl_3$): $\delta = 165.80$, 163.33, 160.65, 149.98, 149.37, 148.54, 144.60, 143.26, 142.09, 141.02, 137.35, 129.30, 128.72, 128.26, 128.18, 128.06, 127.39, 127.17, 124.40, 124.27, 123.04, 120.71, 120.43, 120.32, 102.57, 66.24 ppm; EI-MS: $m/z = 475$ (100, M^+), 315 (45), 237 (55).

Acknowledgments We are grateful to Shanghai Natural Science Foundation (09ZR1409400), Shanghai Committee of Science and Technology of China (10520710100), and the Sino-French Institute of ECNU for financial support.

References

1. Burroughes JH, Bradley DDC, Brown AR, Marks RN, Mackey K, Friend RH, Burn PL, Holmes AB (1990) Nature 347:539
2. Pei J, Liu B, Ni Q, Zhou XH, Lai YH (2001) Acta Chim Sin 59:1712
3. Lupo D, Salbeck J, Schenk H, Stehlin T, Stern R, Wolf A (1998) US Patent 5840217
4. Kreuder W, Lupo D, Salbeck J, Schenk H, Stchlin T (1997) US Patent 5621131
5. Yu WL, Pei J, Huang W, Heeger AJ (2000) Adv Mater 12:828
6. Wu R, Schumm J, Pearson DL, Tour JM (1996) J Org Chem 61:6906
7. Katsis D, Geng YH, Ou JJ, Culligan SW, Trajkovska A, Chen SH, Rothberg L (2002) J Chem Mater 14:1332
8. Wong KT, Chien YY, Chen RT, Wang CF, Lin YT, Chiang HH, Hsieh PY, Wu CC, Chou CH, Su YO, Lee GH, Peng SM (2002) J Am Chem Soc 124:11576
9. Kim YH, Shin DC, Kim SH, Ko CH, Yu HS, Chae YS, Kwon SK (2001) Adv Mater 13:1690
10. Cocherel N, Poriel C, Rault-Berthelot J, Barriere F, Audebrand N, Slawin AMZ, Vignau L (2008) Chem Eur J 14:11328
11. Poriel C, Liang JJ, Rault-Berthelot J, Barriere F, Cocherel N, Slawin AMZ, Horhant D, Virboul M, Alcaraz G, Audebrand N, Vignau L, Huby N, Wantz G, Hirsch L (2007) Chem Eur J 13:10055
12. Sumi K, Konishi G (2010) Molecules 15:7582
13. Wu CC, Lin YT, Chiang HH, Cho TY, Chen CW, Wong KT, Liao YL, Lee GH, Peng SM (2002) Appl Phys Lett 81:577
14. Fournier JH, Maris T, Wuest JD (2004) J Org Chem 69:1762
15. Zhao YP, Zhao CC, Wu LZ, Zhang LP, Tung CH, Pan YJJ (2006) J Org Chem 71:2143
16. Chandrasekaran S, Nagarajan S (2005) Farmaco 60:279
17. Kanagarajan V, Thanusu J, Gopalakrishnan M (2010) Eur J Med Chem 45:1583
18. Patel HS, Patel VK, Dixit BC (2001) Orient J Chem 17:411
19. Umaa K, Ramanathan M, Krishnakumar K, Kannan K (2009) Asian J Chem 21:6674
20. Varga L, Nagy T, Kovesdi I, Benet-Buchholz J, Dorman G, Urge L, Darvas F (2003) Tetrahedron 59:655
21. Haas G, Prelog V (1969) Helv Chim Acta 52:1202
22. Palanki MS, Erdman PE, Gayo FLM, Shevlin GI, Sullivan RW, Goldman ME, Ransone LJ, Bennett BL, Manning AM, Suto MJ (2000) J Med Chem 43:3995
23. Baxendale IR, Schou SC, Sedelmeier J, Ley SV (2010) Chem Eur J 16:89
24. Chandrasekaran S, Nagarajan S (2005) Farmaco 60:279
25. Rawal RK, Tripathi R, Katti SB, Pannecouque C, De CE (2007) Bioorg Med Chem 15:3134

26. Goswami S, Jana S, Dey S, Adak AK (2007) Aust J Chem 60:120
27. Baddar FG, Al-Hajjar FH, El-Rayyes NR (1976) J Heterocycl Chem 13:257
28. Patel PS, Patel SK, Patel KC (2003) Colourage 50:33
29. Tumkevicius S, Dodonova J, Baskirova I, Voitechovicius A (2009) J Heterocycl Chem 46:960
30. Yaziji V, Coelho A, El Maatougui A, Brea J, Loza MI, Garcia-Mera X, Sotelo E (2009) J Comb Chem 11:519
31. Pei J, Ni J, Zhou XH, Cao XY, Lai YH (2002) J Org Chem 67:4924
32. Ingarsal N, Saravanan G, Amutha P, Nagarajan S (2007) Eur J Med Chem 42:517
33. El-Rayyes NRJ (1982) J Heterocycl Chem 19:415
34. Tang CW, Van Slyke SA (1987) Appl Phys Lett 51:913
35. Müllen K, Scherf U (2006) Organic light-emitting devices: synthesis, properties and applications. Wiley-VCH, Weinheim
36. Williams ATR, Winfield SA, Miller JN (1983) Analyst 108:1067
37. Knbin RF, Fletcher AN (1982) J Luminesc 27:455
38. Jeff DD, Jonathan CM, Philip M, Allen JB (1997) J Org Chem 62:530
39. Becke AD (1988) Phys Rev 38:3098
40. Becke AD (1993) J Chem Phys 98:1372
41. Becke AD (1993) J Chem Phys 98:5648
42. Lee C, Yang W, Parr RG (1988) Phys Rev B 37:785
43. Sheldrick GM (2001) SHELXTL, version 6.1. Bruker AXS, Madison